CHAPTER 3

CONFOCAL LASER SCANNING MICROSCOPY STUDY

3.1 The rationale

The objective of this study was to establish the penetration mechanism of propranolol enantiomer from the prepared composite MIP membranes by using confocal laser scanning microscopy (CLSM) which the CLSM result of the composite MIP microparticle both with and without propranolol probe loading and the MIP grafted membrane was compared. By 1-pyrene-butyrate ester of propranolol were used as fluorescent compound model since the previous study showed that *S*-propranolol ester prodrug was enantioselectively released by cellulose grafted with the *S*-MIP more than *R*-propranolol ester prodrug (Bodhibukkana *et al*., 2006) and 1-pyrene-butyric acid is a common fluorescence probe thus the penetration of propranolol ester probe can be followed and the degradation during the transport can be measured by fluorescence microscope. Moreover the advantage of CLSM over HPLC analysis method is that the amount of the drug distributed obtained from CLSM measurement as total drug due to no effect of protein bound and the peak of propranolol and its prodrugs from HPLC are overlapped.

3.2 Experimental

3.2.1 Synthesis of the fluorescent probe

Confocal Laser Scanning Microscope was utilized as a tool to investigate the mechanism of enantioselective release of derivatised propranolol from the MIP composite membrane and the subsequent transport of the enantiomers through excised rat skin (~ 230 μm thickness). Both *R*- and *S*-pyrenebutyryl propranolol esters, which were used as the fluorescence model compounds, were synthesized from *R*- (or *S*-) propranolol and 1-pyrenebutyryl chloride. The latter was obtained by reacting 1-pyrene-butyric acid with thionyl chloride, followed by

extraction of the product using chloroform. The product was recrystallised from hexane before identification was carried out using fluorescence, IR and ^{1}H-NMR spectroscopy. The stability of the derivatized *R*- and *S*-propranolol probes in 80% DMSO (in water) was investigated both at room temperature (30±1^{o}C) and at 37^{o}C, since the compounds were used under these conditions.

3.2.2 The composite MIP membrane embedded with the pyrenebutyryl propranolol ester enantiomer

The microsphere MIP cellulose membranes containing either the *R*- or *S*-pyrenebutyryl propranolol esters were prepared by mixing 1 mg of each fluorescent probe enantiomer with 100 mg of microsphere MIP particulate before casting into cellulose membrane as that for the propranolol loaded membrane. The mean entrapment of *R*-propranolol (24.85±0.35 μg/cm^{2}, n=3) and *S*-propranolol (24.30±0.46 μg/cm^{2}, n=3) probes in the composite membranes were similar, using the measurement protocol same as that for propranolol. In case of permeation study of the microsphere *R*-MIP composite membrane, not contain either propranolol probe in membrane, and composite MIP grafted cellulose membrane racemic propranolol of 24 μg/cm^{2} was loaded in donor phase.

3.2.3 CLSM measurement

The experimental set-up for CLSM measurement of microsphere *S*-MIP composite membrane was carried out in the same way as the skin permeation study described for propranolol at 37^{o}C (see section 2.4.1), except the receptor phase was filled with 2.5 ml of 80% DMSO in water and 300 μl of 80% DMSO in water was applied to the membrane surface within the donor compartment. The permeation of the propranolol probes was determined at different three time intervals (1, 12 and 24 hr) and the experimental set-up for CLSM measurement of composite microsphere *R*-MIP membrane was carried out in the same way of composite microsphere *S*-MIP membrane but the donor phase was applied individual *R*- or *S*-propranolol probe in 80% DMSO in water solution (48 μg/ml, 500 μl). For composite *S*-MIP grafted cellulose membrane, the receptor phase was filled with 2.5 ml of 80% DMSO in water and the donor phase

was loaded with *R*- or *S*-propranolol probe in 80% DMSO in water solution (48 μg/ml, 500 μl). The propranolol probes were investigated for determination of different distribution at four time intervals (1, 6, 12 and 24 hr). At these time points, the membrane and rat skin were promptly recovered and observe the fluorescent marker distribution in the membrane and skin layer under CLSM. Samples of solution were removed from the donor and receiver compartments and these were analyzed for both the respective propranolol probe and 1-pyrene-butyric acid by a fluorescence microscope (Perkin Elmer, Beaconsfield, UK). The quantity of propranolol probe and 1-pyrene-butyric acid was examined by reference to a calibration curve. Additionally, sections of skin and membrane were also cut transversely using a cryomicrotome (Leica, Bensheim, Germany) and examined by CLSM. Each experiment was performed three times independently.

A CLSM (Olympus, Japan) equipped with an Ar-ion laser (Olympus Fluoview FV-300) and Olympus-IX 70 inverted microscope and ×10 or ×20 dry-objectives were used. Optical excitation was carried out using a wavelength of 488 nm and the fluorescence emission was detected at either 630 nm for both the *R*- and *S*-propranolol probes or 580 nm for the hydrolysis product, 1-pyrene-butyric acid. The membrane samples were scanned in 100 μm sections in the direction from the surface in contact with the donor fluid downwards toward the side that was in contact with the skin of composite *R*- or *S*- MIP membrane but the membrane samples were scanned in 60 μm section for composite *S*-MIP grafted cellulose membrane. The rat skin samples were scanned from the epidermal side to dermal side in 230 μm sections. All specimens were x-y scanned towards the z direction at a rate of 0.25 sec/line. The relative intensity (I/I_0) of fluorescence probe and the average intensity (I) of 1-pyrene-butyric acid were plotted as a function of the depth of membrane and/or skin layer, where I_0 was the fluorescent intensity of the membrane/skin specimen measured at time zero.

3.3 Results and Discussion

3.3.1 Identification of the fluorescent probes

Both *R*- and *S*-pyrenebutyryl propranolol esters were accomplished by the

esterification of *R*-(or *S*-) propranolol and 1-pyrenebutyryl chloride in chloroform. The yield of 80% was obtained for both enantiomer probes. The products are yellowish crystalline. For identification, it was found that

IR (KBr) (see Figure 3.1) **:**	3421.20	cm^{-1}	N-H secondary amide
	3052.85	cm^{-1}	C-H, unsaturated
	2966.61	cm^{-1}	C-H, saturated
	2000-1700	cm^{-1}	overtone combination
	1730.88	cm^{-1}	C=O stretching
	1268.83	cm^{-1}	C-C-O stretching
	1103.12	cm^{-1}	C-O-C stretching

^{1}H-NMR (see Figure 3.2):	1.253	ppm	Methyl group of N-isopropyl propranolol part
(in $CDCl_3$)	2.70-2.80	ppm	Methine group of N-isopropyl propranolol part
	4.10-4.26	ppm	Methine group of O-alkyl
	4.80	ppm	N-H group propranolol part
	7.0-8.6	ppm	Aromatic part (broad) (1-pyrene-butyrate+propranolol part)

^{13}C-NMR (see Figure 3.3) :	14.276	ppm	Methyl group of N-isopropyl propranolol part
(in $CDCl_3$)	60.496	ppm	Methylene group of O-alkyl propranolol part
	70.847	ppm	Methine group of O-alkyl propranolol part
	104.79, 120-130	ppm	Aromatic part (1-pyrene-butyrate+propranolol part)
	134.342	ppm	C-C-aromatic 1-pyrene-butyrate part
	153.727	ppm	O-C-aromatic propranolol part
	173.264	ppm	O=C 1-pyrene-butyrate part (ester)

Maximum fluorescence emission	630 nm
excitation	430 nm
Partition coefficient (C log P)	8.46

The results obtained from stability study showed that more than 90% content of both the *R*- and *S*-propranolol fluorescent probes were found after 7 days incubation at room temperature. This indicated that the first-order stability constants (K_H) of the *R*- and *S*-probes which obtained from semi-log scale between amount and time were 0.032 day^{-1} and 0.026 day^{-1}, respectively. The equivalent K_H values at 37^{o}C of the *R*-probe and *S*-probes were found to be similar (calculated as 0.036 day^{-1} and 0.029 day^{-1}, respectively) indicating an acceptable stability of the enantiomers under these conditions.

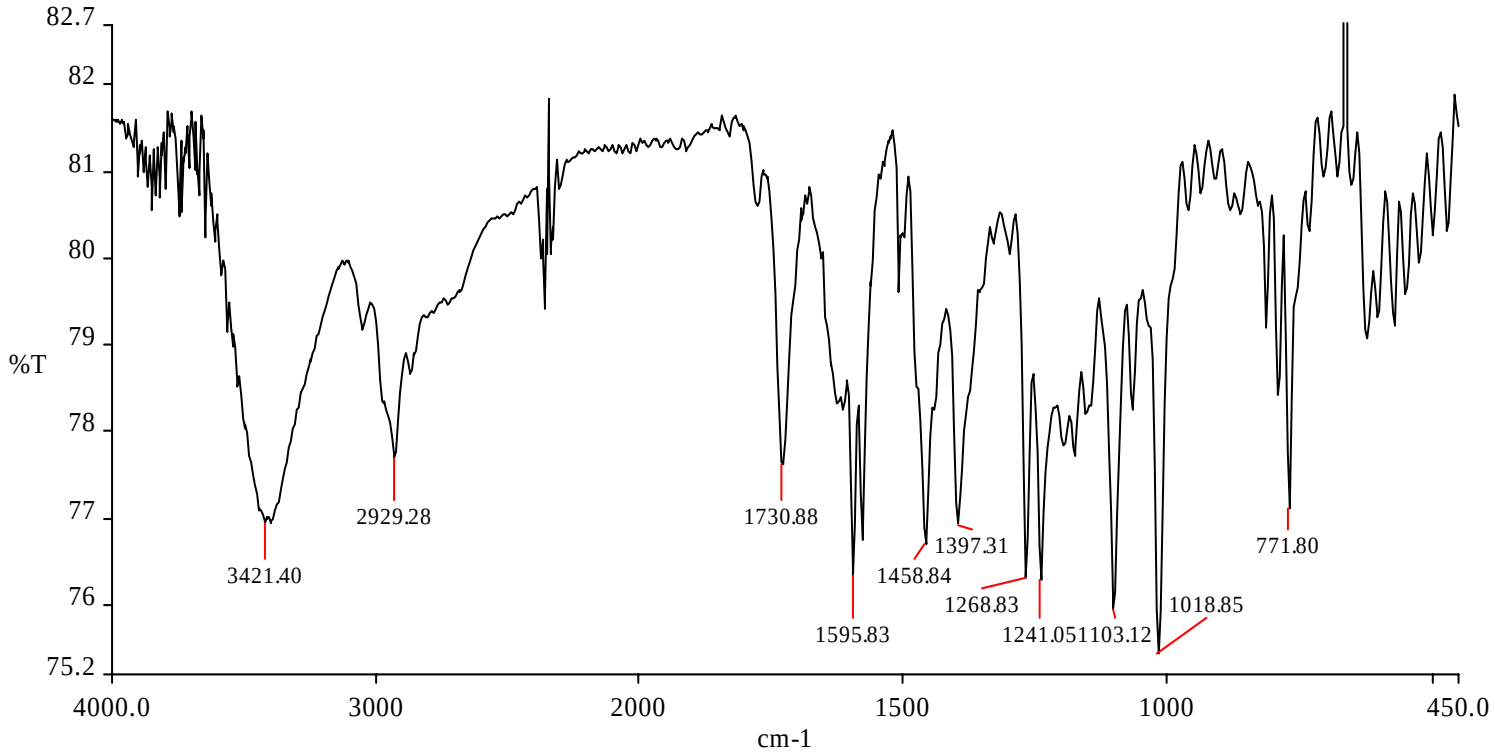

Figure 3.1 IR spectrum of propranolol probe

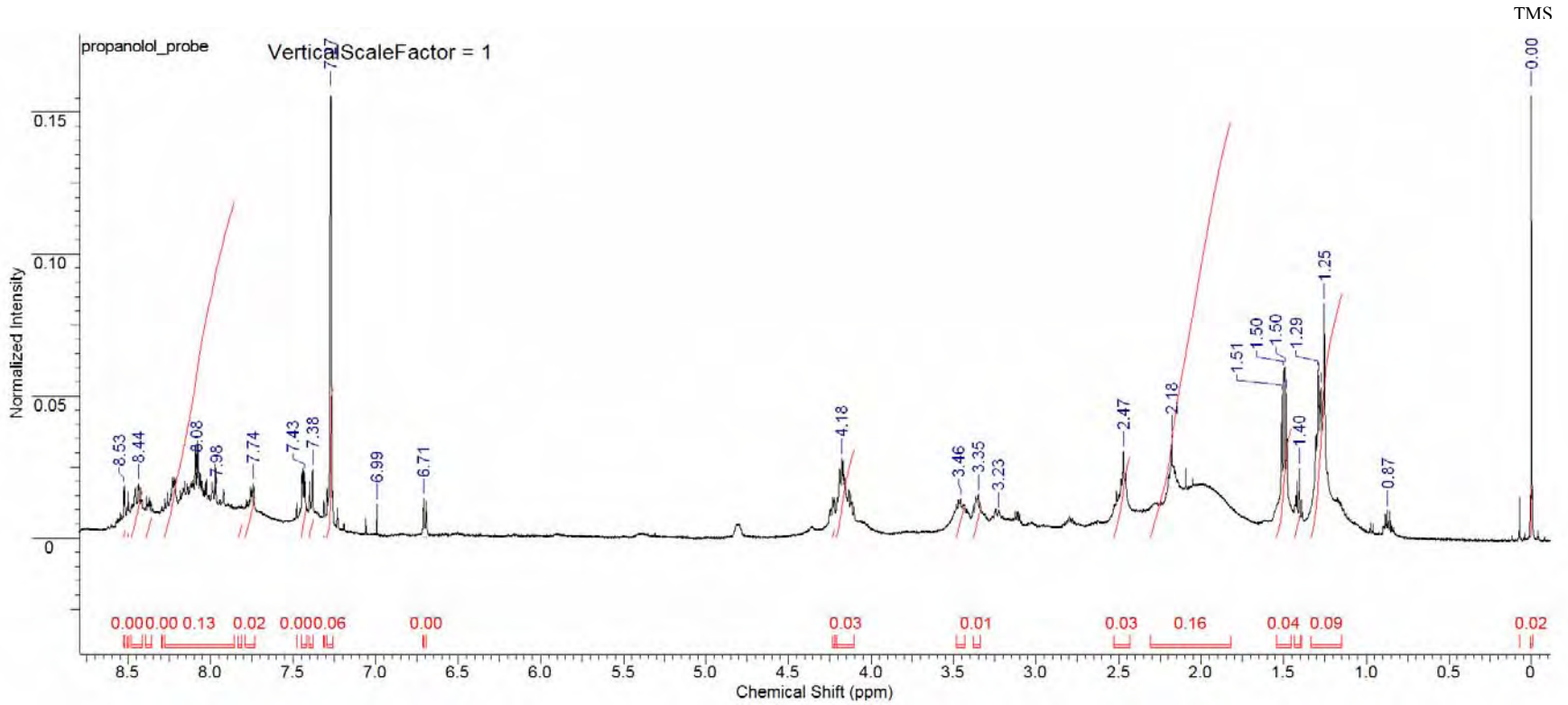

Figure 3.2 ^{1}H-NMR of propranolol probe

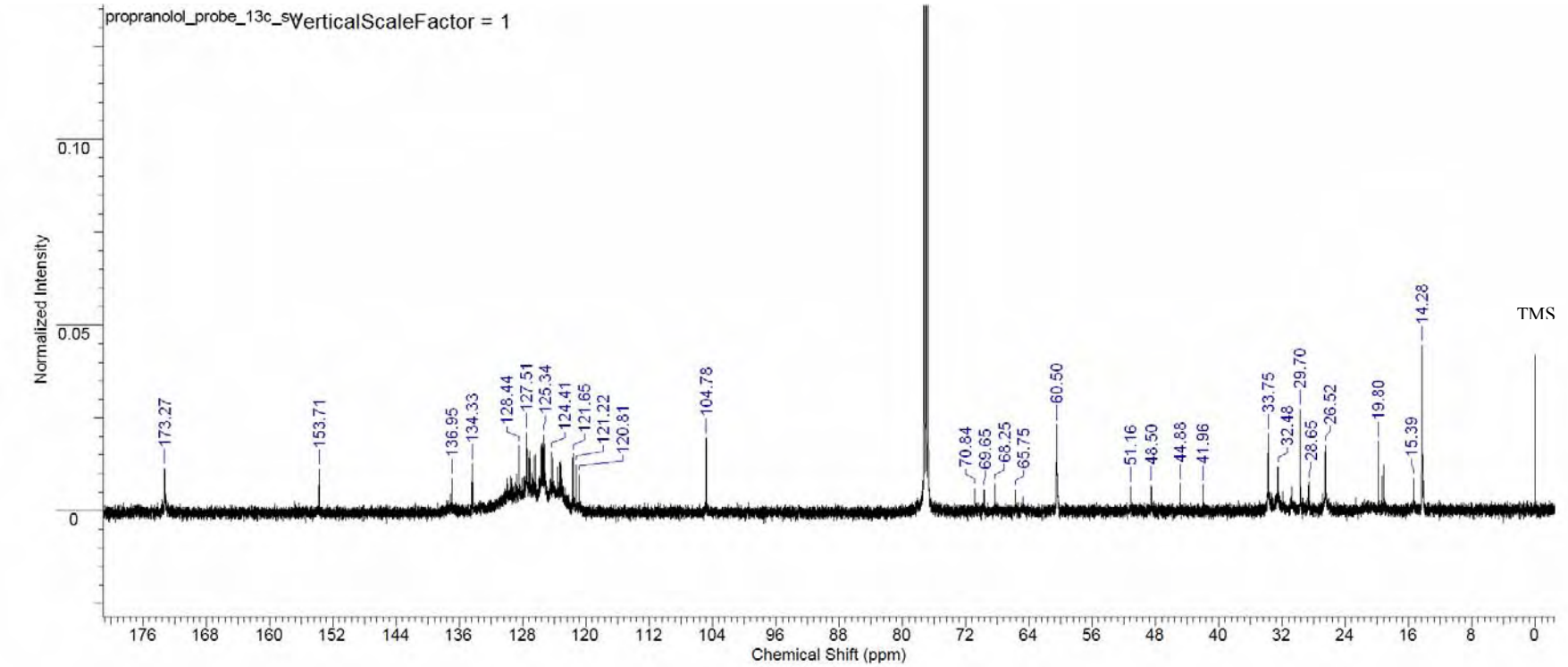

Figure 3.3 ^{13}C-NMR of propranolol probe

3.3.2 The CLSM study

In order to investigate the mechanism of selective release of the propranolol enantiomers from the microsphere *S*-MIP composite BC membrane, the membranes were fabricated in the presence of either the *R*- or *S*-propranolol enantiomer labeled with the 1-pyrene butyric acid probe. It was reported previously that the propranolol ester prodrugs were released enantioselectively from a BC membrane which had been grafted to a *S*-propranolol imprinted polymer layer, produced from the same materials as those employed in the present study (Bodhibukkana *et al*., 2006). In that study the *S*-isomer was released at a faster rate than the *R*-isomer. The intensity of fluorescence emission of the membrane and rat-skin at 630 nm, the wavelength used to monitor the *R*- and *S*-propranolol esters was found to be very low. The CLSM scan provided a 2-D image of the coupled propranolol probe and of 1-pyrene-butyric acid, a product derived from 1-pyrenebutyryl propranolol enantiomers by hydrolysis affected by enzymes in the skin.

Figure 3.4 shows the relative intensity (I/I_0) of the *R*- and *S*-enantiomer of fluorescence probe detected in either the membrane or rat skin layer at different depth after treatment for 1, 12 or 24 hr. The amounts of *R*- and *S*-propranolol probe enantiomer detected in donor and receiving phase as well as the amounts of 1-pyrene-butyric acid that was found in rat skin samples at different time points are shown in Table 3.1. The results showed that mean I/I_0 of either *R*- or *S*-propranolol fluorescent probes at most depth of the membrane after treatment for 1 hr was about 1 and that there was no statistical difference between I/I_0 values of the *R*- and *S*-isomer in the membranes at these time points. A greater amount of the *S*-propranolol fluorescent probe in comparison to *R*-probe was detected in the donor solution after 1 hr due to diffusion of the probes from the membrane into the applied donor phase. The diffusion of the probes through the stratum corneum is clearly proceeding during this time (Figure 3.4) and after 1 hr the *S*-enantiomer can be determined in higher concentration than the *R*-enantiomer in the lower layers of the skin. It was found that the fluorescent intensity of both propranolol analogues within the membrane, 12 hr after initial application was markedly greater than that before the solvent was applied (Figure 3.4). Before treatment of the membrane with solvent the propranolol probes are included in the dry state within the MIP particles in the composite membrane, and this is poorly

detected by CLSM. After solvent has diffused into the membrane and the propranolol probes are dissolved the fluorescence can be determined by CLSM. More of the *R*-probe was detected within the membrane after 12 hr than the *S*-probe, whilst more *S*-probe was present in the donor phase after this time, having been selectively extracted. At 24 hr an *S/R* selectivity of permeation into lower skin layers was apparent for the probe, particularly at depths closer to the dermal side. A significantly higher concentration of the *S*-enantiomer had diffused from the membranes across the skin after 24 hr in comparison to the *R*-enantomer (Table 3.1).

Figure 3.5 shows the typical photomicrographs of the distribution of *R*- and *S*-fluorescence probes within rat skin samples after treatment for 1, 12 or 24 hr. At all time points the fluorescence from either probe was more apparent within the dermal rather than the epidermal layers. In addition at most time points it was apparent that the intensity of fluorescence of the *S*-propranolol probe within the dermal area of the skin. Facilitated release of the template isomer of microsphere *S*-MIP composite membrane occurs after the racemate is loaded into the composite membrane. The mechanism underlying this controlled release of the template enantiomer from the microsphere *S*-MIP composite membrane may be explained by the non-covalent interaction of this enantiomer with the MIP binding site in the microsphere *S*-MIP composite membrane and disruption of this binding with solvent that causes the release of the isomer into the receiving or donor phases. The binding of the template molecule to the MIP may result in a structural change to the polymer, which perhaps results in polymer shrinkage or swelling, when in the dry or wet state (Suedee *et al.,* 2002). Such a phenomenon might contribute to the increased mobility of the template molecule at the binding site, leading to a more rapid release of the template molecule from the membrane. As discussed previously esterases are present in the skin which will enhance the hydrolysis of a variety of different ester compounds. Some ester prodrugs which are chiral compounds are widely used for the enhancement of percutaneous penetration and these have been reported to show stereoselective hydrolysis in skin (Ahmed *et al.,* 1997). Figure 3.4 shows the fluorescence intensity of 1-pyrene-butyric detected at different depths of skin layer after permeation of *R*- or *S*-propranolol probe for 1, 12 or 24 hr and the amount of transport to the receptor compartment after the same time intervals is shown in Table 3.1. The 1-pyrene-butyric acid is derived from the hydrolysis of the propranolol ester fluorescence probe by the enzymes in rat skin. The hydrolysis of the *R*-propranolol probe was found to be markedly higher than that of

the *S*-propranolol at depths between 10-20 μm after 12 h of permeation, but at 24 h the conversion of either *R*- or *S*-enantiomer probes to 1-pyrene-butyric acid was not significantly different (Figure 3.4). The rate of hydrolysis of the *R*- and *S*-propranolol probes due to the enzyme in the excised rat skin was calculated as 7.96 and 6.84 day^{-1}, respectively.

Table 3.1 The concentration of *R*- and *S*-propranolol probe and 1-pyrene-butyric acid detected in donor and receiver phases after application of solvent to a composite MIP microsphere membrane in the pyrene of propranolol probe placed on isolated rat epidermal sections (mean ± S.D., n = 3). The composite MIP membrane of this type was prepared by integration of *S*-propranolol imprinted polymer.

Time (h)	Enantiomer	The probe		1-pyrene-butyric acid
		Donor (μg/ml)	Receiver (μg/ml)	Receiver (μg/ml)
1	*R*	0.65 ± 0.18	0.87 ± 0.22	ND
	S	1.01 ± 0.21	0.91 ± 0.12	ND
	S/R ratio	1.76 ± 0.63	1.06 ± 0.20	ND
12	*R*	1.78 ± 0.36	1.41 ± 0.54	1.10 ± 0.15
	S	2.91 ± 0.34	2.03 ± 0.55	0.73 ± 0.10
	S/R ratio	1.70 ± 0.35	1.49 ± 0.22	0.68 ± 0.05
24	*R*	3.93 ± 0.48	2.64 ± 0.11	1.34 ± 0.04
	S	4.79 ± 0.40	3.13 ± 0.44	1.14 ± 0.46
	S/R ratio	1.24 ± 0.35	1.29 ± 0.54	0.84 ± 0.18

ND: non detectable

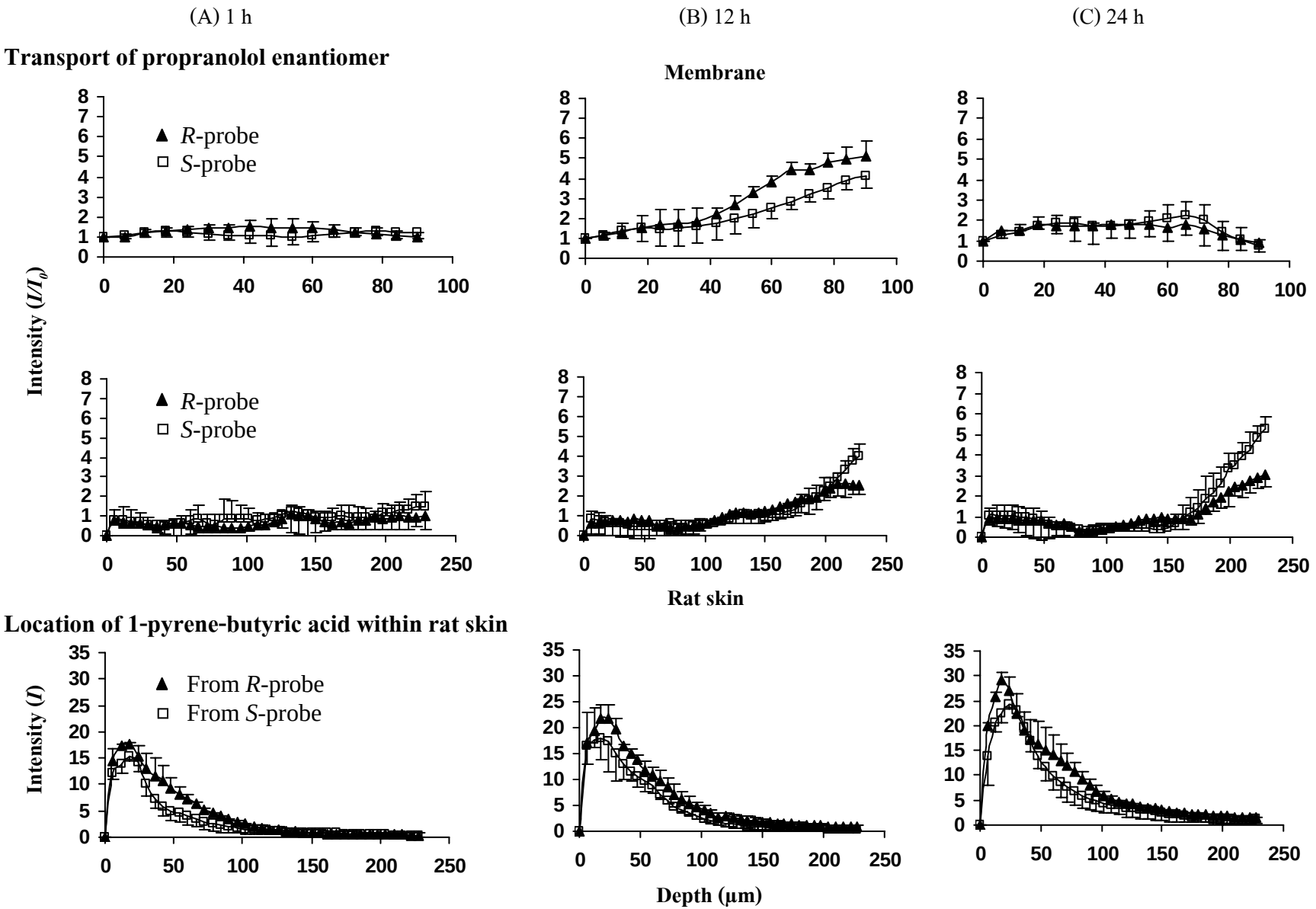

Figure 3.4 Distribution of the pyrenebutyrate ester of propranolol and pyrenebutyric acid in the membrane and rat skin at 1, 12 and 24 hr of the composite MIP microparticles membrane in the presence of propranolol probe. The composite MIP membrane of this type was prepared by integration of *S*-propranolol imprinted polymer (mean±SD., n=3).

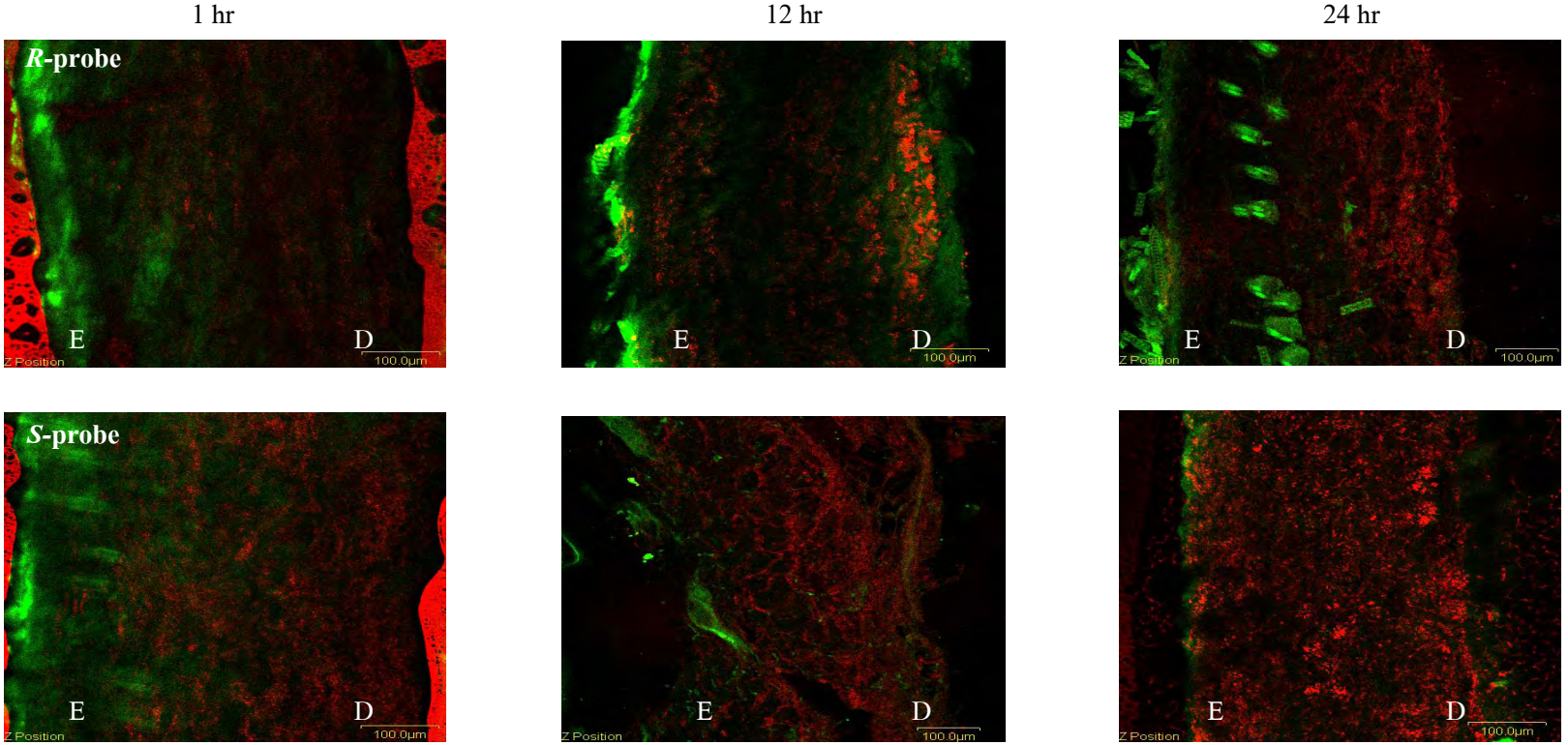

Figure 3.5 CLSM image showing distribution of *R* and *S*-propranolol fluorescent probe (red) in rat skin specimen (cross section) after treatment for 1, 12 and 24 hr overlaid with blank (control) rat skin (green) of the composite MIP microparticles membrane; E= epidermal side, D= dermal side. The composite MIP membrane of this type was prepared by integration of *S*-propranolol imprinted polymer.

For composite microsphere *R*-MIP membrane, the plot of the relative intensity of fluorescence (I/I_0) as a function of depth of the specimen is shown in Figure 3.6. For membrane, the *R*-propranolol probe was more diffused into the membrane at 1 hr than *S*-propranolol probe, the intensity of the *R*-probe was higher than the intensity of the *S*-probe at 12 hr, but the intensity of the *R*- and *S*-probes in the membrane decreased at 24 hr (the amount of *R*-probe and *S*-probe in the surface of the tested membranes are 24.04 ± 0.35 μg/cm^2 and 24.49 ± 0.41 μg/cm^2, respectively). In contrast, in the rat skin, the intensity of either *R*- or *S*-probe was gradually increased with time, and the *R*-probe transited across the rat skin higher than *S*-probe at every time point. Moreover, in the receiving phases, the amount of the *R*-probe was found to be higher than that of the *S*-probe at 12 and 24 hr (Table 3.2) but at 1 hr, the amount of the *R*-probe can not be detected and the amount of the *R*-probe was lower than the *S*-probe at 1, 12 and 24 hr in the donor phase. The distribution of the *R*- and *S*-fluorescent probes in the rat skin after treatment, it can be seen that *R*-propranolol prodrug can penetrate into the rat skin samples more than *S*-propranolol prodrug. And, a higher amount of the probe was found at the deeper skin layer.

The pyrene butyric acid found in the rat skin was derived from hydrolysis of a propranolol ester prodrug by the enzyme in the rat skin. The skin hydrolysis of the *R*-probe prodrug was higher than that of the *S*-probe prodrug at 24 hr of penetration only, but that at 1 and 12 hr no stereoselective hydrolysis occurred during penetration of the prodrugs. The previous study by Ahmed *et al.,* 1997 also showed the stereoselectivity for skin hydrolysis of the ester prodrugs, isovaleryl propranolol and cyclopropranoyl propranolol when delivered through the mouse skin. This confirms the hydrolysis result obtained in the present study.

From the results obtained, the mechanism of enantioselective diffusion by the composite *R*-MIP cellulose membrane can be concluded as followed, the propranolol ester binds to the binding site of the MIP particles in the membrane when the propranolol probe was initial applied especially the *R*-probe. The propranolol probes diffuse into the MIP particles, presumably at imprint sites, and which the release of the *R*-probe was higher than that of the *S*-probe. The *S*-probe remaining in the donor phase and transported across the rat skin hence low *R/S* selectivity in rat skin at 12 hr after 12 hr, and the enantioselectivity in rat skin increase again. This is because of the transport of propranolol probe from the donor phase higher at long time. Apart from this, the skin hydrolysis of the *R*-probe prodrug was higher than that of the S-probe prodrug. So, the

enantioselectivity of transport is likely to be the result of the affinity of MIP in the cellulose membrane and facilitation release of the MIP composite membrane. To see the distribution of *R*- and *S*-propranolol probe to confirm the results of this experiment, the intensity of *R*-probe was found to be higher than the *S*-probe in the dermal more than epidermal layers at all time (Figure 3.7).

Table 3.2 The concentration of *R*- and *S*-propranolol probe and 1-pyrene-butyric acid detected in donor and receiving phases after application of 48 μg/ml of propranolol probe to a composite microsphere membrane placed on isolated rat epidermal sections (mean ± S.D., n = 3). The composite MIP membrane of this type was prepared by integration of *R*-propranolol imprinted polymer.

Time (h)	Enantiomer	The probe		1-pyrene-butyric acid
		Donor (μg/ml)	Receiver (μg/ml)	Receiver (μg/ml)
1	*R*	38.17 ± 0.77	ND	ND
	S	38.83 ± 0.11	ND	ND
	R/S ratio	0.93 ± 0.02	ND	ND
12	*R*	26.32 ± 0.92	1.02 ± 0.21	1.06 ± 0.61
	S	29.97 ± 0.42	0.95 ± 0.19	0.63 ± 0.10
	R/S ratio	0.88 ± 0.04	1.08 ± 0.12	1.67 ± 0.21
24	*R*	22.69 ± 0.60	1.44 ± 0.59	1.28 ± 0.50
	S	26.55 ± 0.61	1.16 ± 0.37	1.01 ± 0.34
	R/S ratio	0.85 ± 0.09	1.24 ± 0.44	1.26 ± 0.27

ND: non detectable

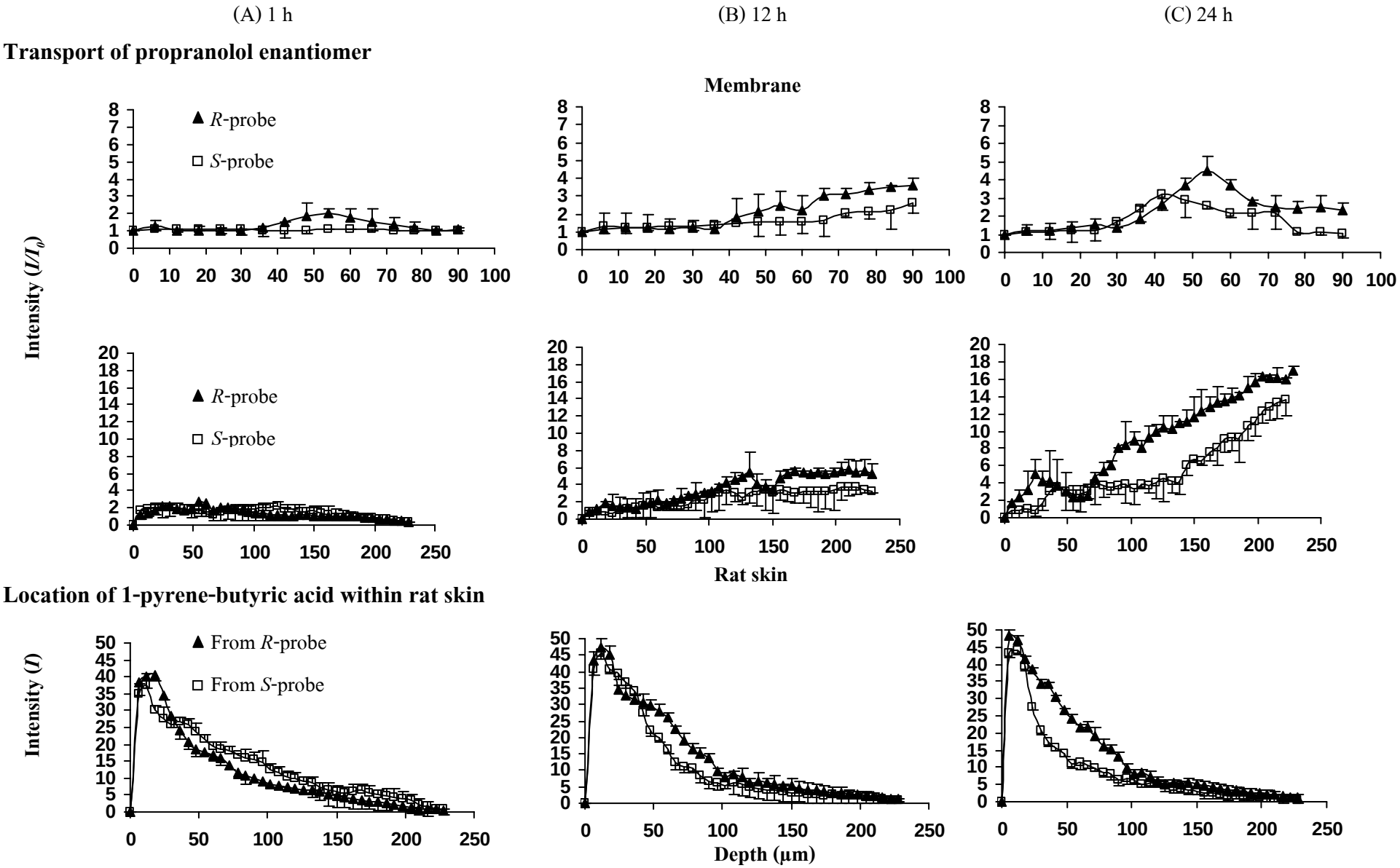

Figure 3.6 Distribution of the pyrenebutyrate ester of propranolol and pyrenebutyric acid in the membrane and rat skin at 1, 12 and 24 hr of the composite MIP microparticles membrane after application of 48 μg/ml of propranolol probe to donor phase. The composite MIP membrane of this type was prepared by integration of *R*-propranolol imprinted polymer (mean±SD., n=3).

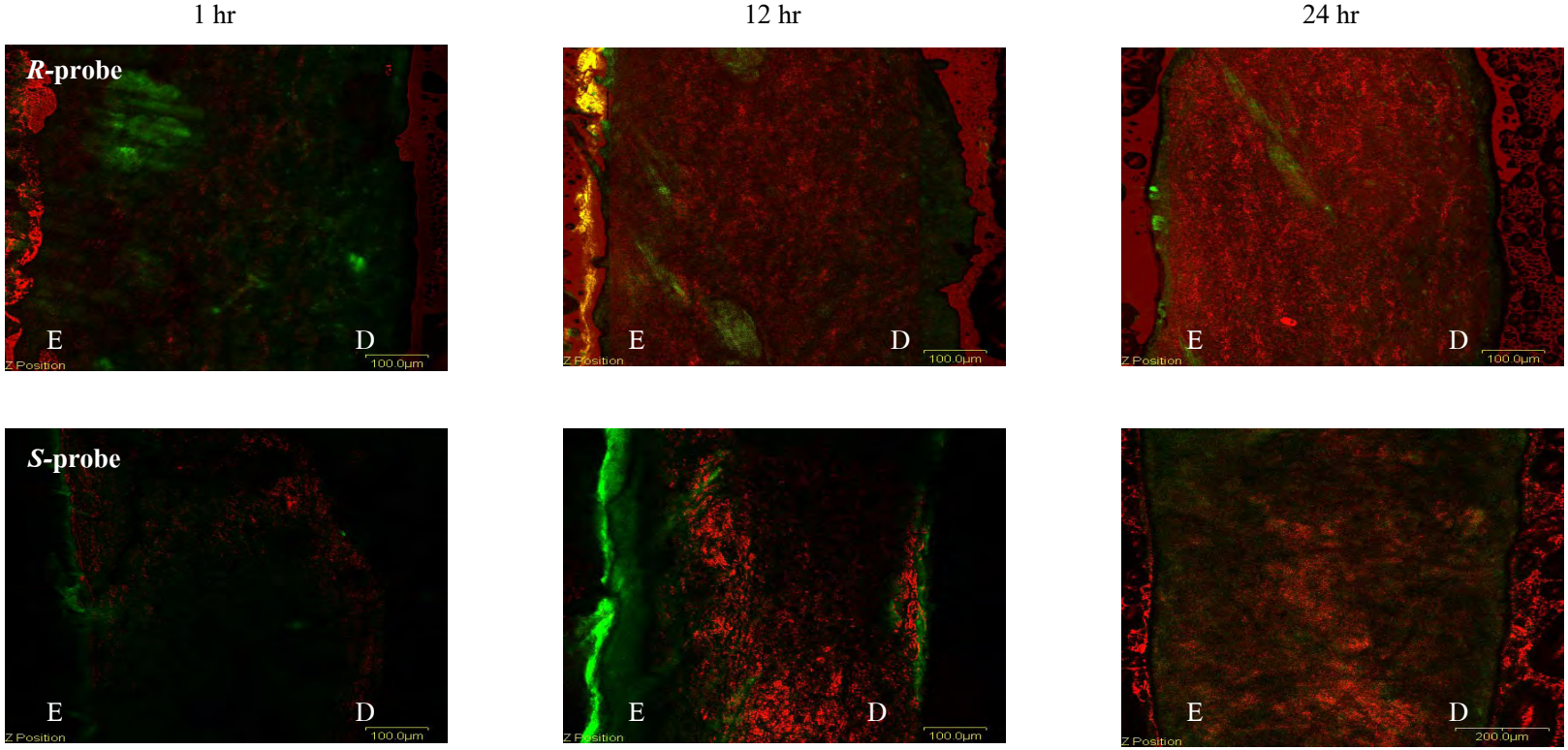

Figure 3.7 CLSM image showing distribution of *R* and *S*-propranolol fluorescent probe (red) in rat skin specimen (cross section) after treatment for 1, 12 and 24 h overlaid with blank (control) rat skin (green) of the composite MIP microparticles membrane; E= epidermal side, D= dermal side. The composite MIP membrane of this type was prepared by integration of *R*-propranolol imprinted polymer.

Further, the relative intensity of fluorescence (I/I_0) as a function of depth of the MIP grafted cellulose membrane was plotted. As seen in Figure 3.8, the *R*-and *S*-propranolol probe were spread all over the membrane at 1 hr, the intensity of the *S*-probe was higher than the intensity of the *R*-probe at 6, 12 and 24 hr (the amount of *R*-probe and *S*-probe in the surface of the tested membranes are 24.04±0.35 μg/cm^2 and 24.49±0.41 μg/cm^2, respectively). The fluorescence of the *S*-probe was higher at deeper membrane layers when increase time interval. This result suggests that the complexation and deconplexation between the *S*-probe and recognition site was obtained step by step at longer times. However, in the rat skin sample, the *S*-probe penetrated across the rat skin higher than *R*-probe at 12 and 24 hr and no significantly difference between the fluorescence intensity of *R*- or *S*-probe at 1 and 6 hr (Figure 3.8). Moreover, in the donor phase, the amount of *R*-probe was higher than the *S*-probe at every time point (see Table 3.3).

For degradation, pyrene butyric acid, the skin hydrolysis of the *R*-probe was higher than the *S*-probe at 6 and 12 hr and these is no significantly difference of *R*- and *S*-probe of skin hydrolysis during penetration at 1 and 24 hr (Figure 3.8). The hydrolysis of *R*-probe detected from receiving phase was found to be higher than that of *S*-probe at 6 and 12 hr but at 24 hr. No difference from conversion from propranolol ester probe between *R*- or *S*-isomer was found (see the data in Table 3.3). Since the amount of *S*-probe was higher than *R*-probe so that the hydrolysis from *S*-probe was increased. From this experiment, the mechanism of enantioselective penetration by the MIP grafted cellulose membrane can be concluded that the propranolol probe interacts with recognition sites and rebind by the solvent, which the interaction with recognition site occurs step by step through the MIP membrane. The *S/R* selectivity in rat skin was increased after 12 hr of permeation but was low at initial time, because the *S*-probe interacts with recognition site was delayed. But *S/R* selectivity in the receiving phase was increased over 24 hr of permeation (see Table 3.3). Thus, the enantioselectivity of transport is related to the affinity of MIP in the membrane. To confirm the distribution of *R*- and *S*-fluorescent probe penetrated into the rat skin after the treatment. The intensity of the *S*-probe was higher than the *R*-probe and the fluorescence of either probe was in the dermal rather than the epidermal layers at every time point (Figure 3.9). Table 3.4 shows %amount of *R*-and *S*-propranolol probe detected in various phases of the different composite MIP cellulose membranes. For the MIP grafted membrane, %amount of *S*-

probe was lower than that of *R*-probe in donor phase, whilst %amount of *S*-probe was higher than the *R*-probe in membrane, rat skin and receiving phase. The *S*-probe penetrates into receiving phase more than *R*-probe over 24 hr. The amount of probe in rat skin at 24 hr was lower than that at 12 hr. This may be because the saturation of binding site of the MIP in membrane was occurred. For composite MIP particle membrane, %amount of *R*-probe increased with time in membrane, rat skin and receiving phase, but %amount of *R*-probe was lower than the *S*-probe in donor phase. In composite microsphere *S*-MIP membrane, %amount of *S*-probe was found to be higher than the *R*-probe in donor phase, membrane, rat skin and receiving phase at 12 and 24 hr of application but that at 12 hr, %amount of *R*-probe in the membrane was higher than the *S*-probe because the *S*-probe interact with binding site which can not be detected by CLSM. And, there is no statistical difference in terms of fluorescent intensity of *R*- and *S*-probe in each compartment at 1 hr for all the composite MIP cellulose membranes.

Table 3.3 The concentration of *R*- and *S*-propranolol probe and 1-pyrene-butyric acid detected in donor and receiver phases after application of solvent to a MIP grafted cellulose membrane placed on isolated rat epidermal sections (mean ± S.D., n = 3)

Time (h)	Enantiomer	The probe		1-pyrene-butyric acid
		Donor (μg/ml)	Receiver (μg/ml)	Receiver (μg/ml)
1	*R*	34.75 ± 0.63	ND	ND
	S	34.43 ± 0.43	ND	ND
	S/R ratio	0.99 ± 0.03	ND	ND
6	*R*	28.17 ± 0.85	0.45 ± 0.11	0.46 ± 0.11
	S	25.90 ± 0.80	0.81 ± 0.14	0.21 ± 0.10
	S/R ratio	0.92 ± 0.06	1.78 ± 0.19	0.44 ± 0.13
12	*R*	21.32 ± 0.62	0.98 ± 0.12	1.01 ± 0.42
	S	16.17 ± 0.91	1.59 ± 0.75	0.73 ± 0.16
	S/R ratio	0.75 ± 0.02	1.60 ± 0.39	0.71 ± 0.14
24	*R*	17.31 ± 0.93	1.70 ± 0.58	1.42 ± 0.23
	S	14.05 ± 0.97	1.95 ± 0.43	1.39 ± 0.51
	S/R ratio	0.81 ± 0.10	1.35 ± 0.48	0.94 ± 0.20

ND: non detectable

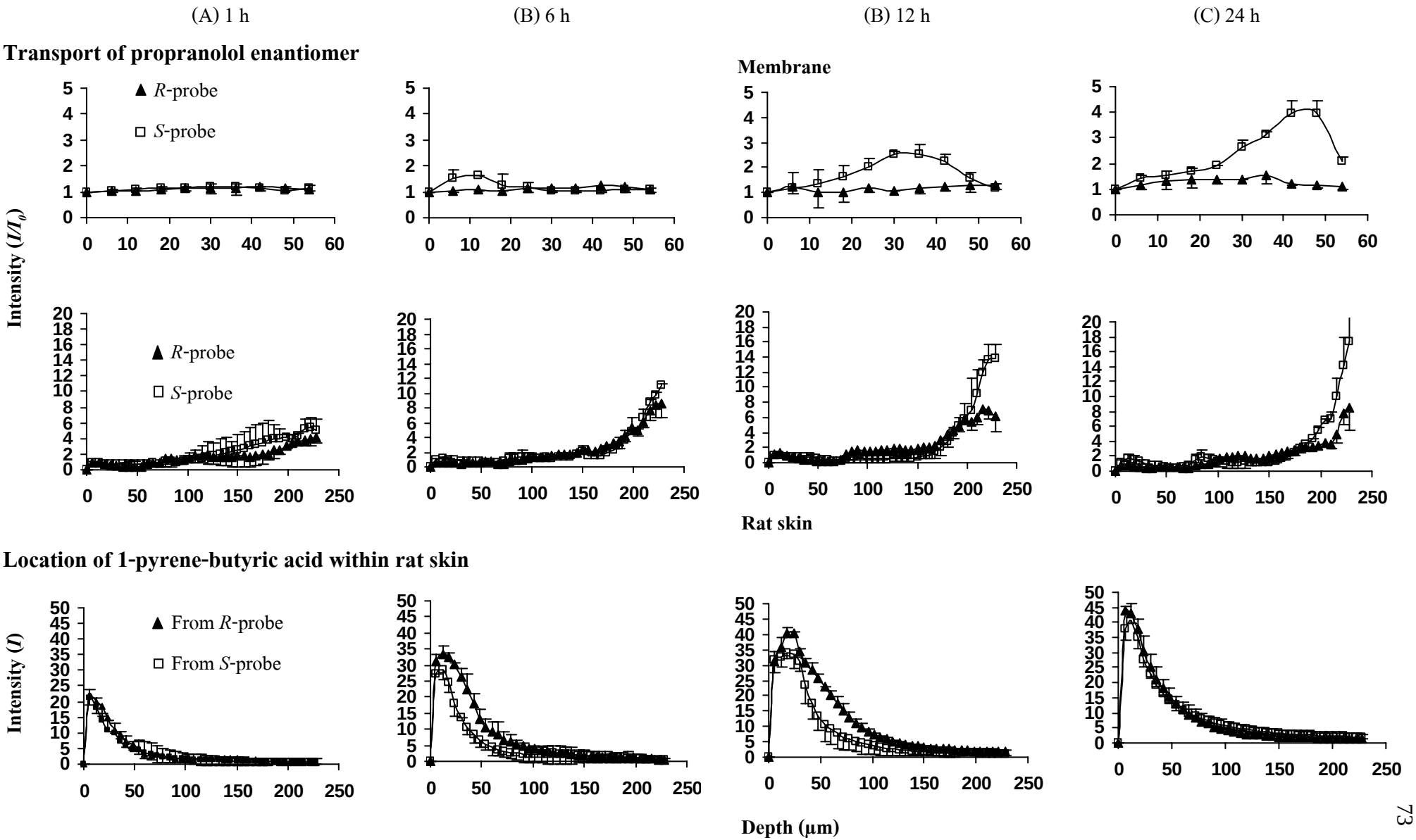

Figure 3.8 Distribution of the pyrenebutyrate ester of propranolol and pyrenebutyric acid in the membrane and rat skin at 1, 6, 12 and 24 hr of composite MIP grafted membrane (mean±SD., n=3).

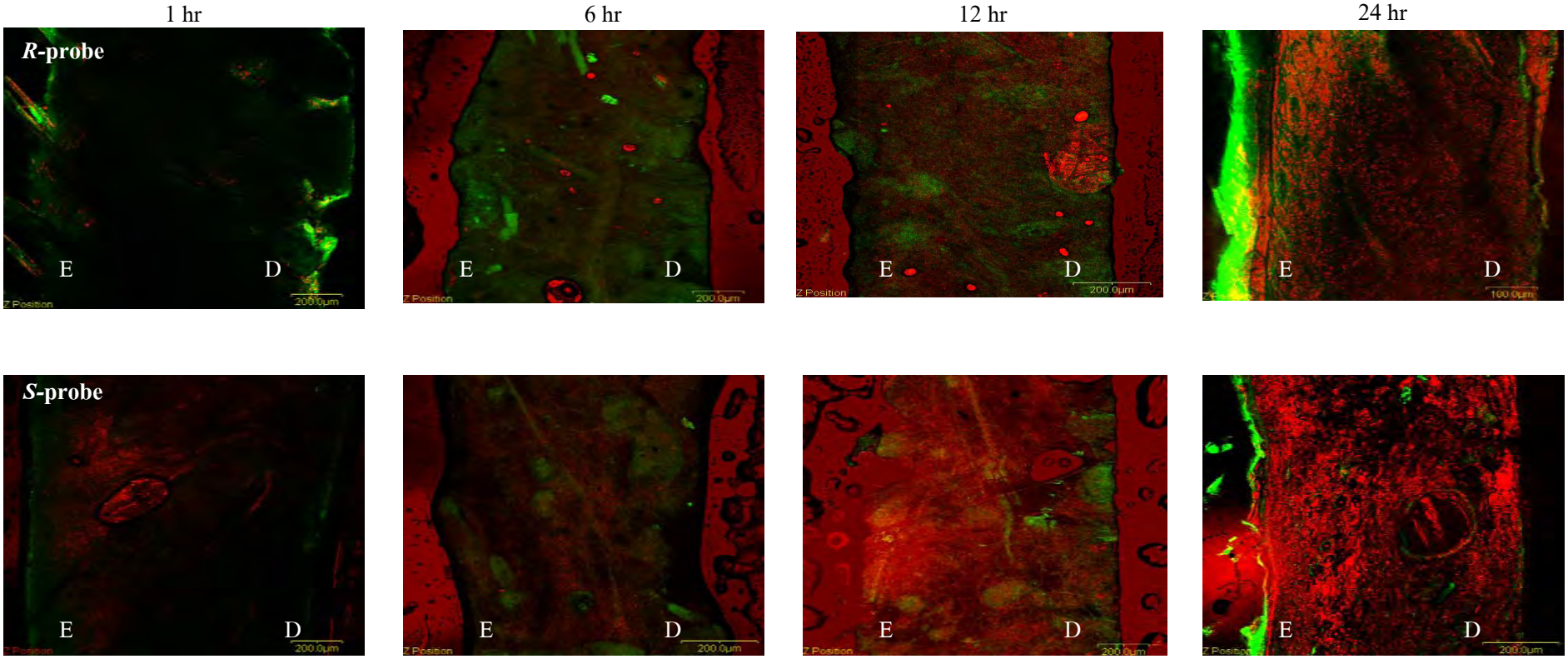

Figure 3.9 CLSM image showing distribution of *R* and *S*-propranolol fluorescent probe (red) in rat skin specimen (cross section) after treatment for 1, 12 and 24 hr overlaid with blank (control) rat skin (green) of composite MIP grafted membrane; E= epidermal side, D= dermal side

Table 3.4 The %amount of R-and S-propranolol probe in each compartment from composite MIP membrane at different time

Membrane	probe	time(hr)	%amount in donor phase	%amount in membrane	%amount in rat skin	%amount in receiving phase
Grafting	*R*-probe	1	72.41±1.01	11.24±0.21	16.35±0.21	ND
S-MIP		6	58.7±0.96	11.76±0.11	19.97±0.24	9.57±0.27
(load in donor		12	44.41±1.04	13.69±0.64	21.13±0.62	20.77±0.63
phase)		24	36.06±0.67	14.15±0.35	17.29±0.14	32.50±0.64
	S-probe	1	71.74±0.71	12.68±0.59	15.58±0.34	ND
		6	53.96±0.85	13.06±0.31	22.26±0.11	10.72±0.12
		12	33.7±0.27	15.23±0.22	26.83±0.53	24.24±0.37
		24	29.27±0.45	16.32±0.49	19.58±0.22	34.83±0.43
Casting	*R*-probe	1	79.53±0.13	9.95±0.93	10.52±0.31	ND
R-MIP		12	54.83±1.04	10.05±0.41	13.35±0.43	21.77±0.83
(load in donor		24	47.27±1.94	11.09±0.74	13.20±0.51	28.44±1.05
phase)	*S*-probe	1	80.90±0.11	7.25±0.75	11.85±0.45	ND
		12	62.45±1.51	8.52±0.35	12.55±0.12	16.48±0.84
		24	55.32±1.53	9.35±0.22	12.69±0.23	22.64±1.20
S-MIP	*R*-probe	1	0.89±0.14	11.72±0.15	13.39±0.21	9.94±0.09
(load in		12	2.42±0.23	17.34±0.11	19.34±0.12	26.60±0.19
membrane)		24	5.37±0.25	14.36±0.14	25.47±0.18	45.26±0.14
	S-probe	1	1.37±0.20	12.38±0.19	11.86±0.11	10.31±0.11
		12	3.97±0.18	15.58±0.30	22.73±0.19	31.31±0.24
		24	6.53±0.19	15.64±0.20	26.60±0.10	48.86±0.10